

# Transmitted/Founder Hepatitis C Viruses Induce Cell-Type- and Genotype-Specific Differences in Innate Signaling within the Liver

Angela M. Mitchell,<sup>a,b</sup> Amy E. L. Stone,<sup>a,b</sup> Linling Cheng,<sup>b</sup> Kimberly Ballinger,<sup>c</sup> Michael G. Edwards,<sup>d</sup> Mark Stoddard,<sup>e</sup> Hui Li,<sup>e</sup> Lucy Golden-Mason,<sup>a,b</sup> George M. Shaw,<sup>e</sup> Salman Khetani,<sup>c</sup> Hugo R. Rosen<sup>a,b,f</sup>

Integrated Department of Immunology, University of Colorado Denver and National Jewish Health, Denver, Colorado, USA<sup>a</sup>; Division of Gastroenterology and Hepatology, Hepatitis C Center, Department of Medicine, University of Colorado Denver, Denver, Colorado, USA<sup>b</sup>; Mechanical and Biomedical Engineering, Colorado State University, Fort Collins, Colorado, USA<sup>c</sup>; Department of Medicine, Division of Pulmonary Sciences and Critical Care Medicine, University of Colorado Denver, Aurora, Colorado, USA<sup>d</sup>; Perelman School of Medicine, University of Pennsylvania, Philadelphia, Pennsylvania, USA<sup>e</sup>; Denver Veteran's Affairs Medical Center, Denver, Colorado, USA<sup>f</sup>

**ABSTRACT** Hepatitis C virus (HCV) infection leads to persistence in the majority of cases despite triggering complex innate immune responses within the liver. Although hepatocytes are the preferred site for HCV replication, nonparenchymal cells (NPCs) can also contribute to antiviral immunity. Recent innovations involving single-genome amplification (SGA), direct amplicon sequencing, and phylogenetic inference have identified full-length transmitted/founder (T/F) viruses. Here, we tested the effect of HCV T/F viral RNA (vRNA) on innate immune signaling within hepatocytes and NPCs, including the HepG2 and Huh 7.5.1 cell lines, a human liver endothelial cell line (TMNK-1), a plasmacytoid dendritic cell line (GEN2.2), and a monocytic cell line (THP-1). Transfection with hepatitis C T/F vRNA induced robust transcriptional upregulation of type I and III interferons (IFNs) within HepG2 and TMNK-1 cells. Both the THP-1 and GEN2.2 lines demonstrated higher type I and III IFN transcription with genotype 3a compared to genotype 1a or 1b. Supernatants from HCV T/F vRNA-transfected TMNK-1 cells demonstrated superior viral control. Primary human hepatocytes (PHH) transfected with genotype 3a induced canonical pathways that included chemokine and IFN genes, as well as overrepresentation of RIG-I (DDX58), STAT1, and a Toll-like receptor 3 (TLR3) network. Full-length molecular clones of HCV induce broad IFN responses within hepatocytes and NPCs, highlighting that signals imparted by the various cell types within the liver may lead to divergent outcomes of infection. In particular, the finding that HCV genotypes differentially induce antiviral responses in NPCs and PHH might account for relevant clinical-epidemiological observations (higher clearance but greater necroinflammation in persistence with genotype 3).

**IMPORTANCE** Hepatitis C virus (HCV) has become a major worldwide problem, and it is now the most common viral infection for which there is no vaccine. HCV infection often leads to persistence of the virus and is a leading cause of chronic hepatitis, liver cancer, and cirrhosis. There are multiple genotypes of the virus, and patients infected with different viral genotypes respond to traditional therapy differently. However, the immune response to the virus within the liver has not been fully elucidated. Here, we determined the responses to different genotypes of HCV in cell types of the liver. We found that the immune response varied according to both cell type and HCV genotype, leading to a more pronounced induction of inflammatory pathways after exposure to certain genotypes. Therefore, inflammatory pathways that are being robustly activated by certain HCV genotypes could lead to more severe damage to the liver, inducing diverse outcomes and responses to therapy.

Received 18 December 2014 Accepted 8 January 2015 Published 24 February 2015

**Citation** Mitchell AM, Stone AEL, Cheng L, Ballinger K, Edwards MG, Stoddard M, Li H, Golden-Mason L, Shaw GM, Khetani S, Rosen HR. 2015. Transmitted/founder hepatitis C viruses induce cell-type- and genotype-specific differences in innate signaling within the liver. *mBio* 6(2):e02510-14. doi:10.1128/mBio.02510-14.

**Editor** Diane E. Griffin, Johns Hopkins University School of Public Health

**Copyright** © 2015 Mitchell et al. This is an open-access article distributed under the terms of the [Creative Commons Attribution-Noncommercial-ShareAlike 3.0 Unported license](https://creativecommons.org/licenses/by-nc-sa/4.0/), which permits unrestricted noncommercial use, distribution, and reproduction in any medium, provided the original author and source are credited.

Address correspondence to Hugo R. Rosen, [hugo.rosen@ucdenver.edu](mailto:hugo.rosen@ucdenver.edu).

This article is a direct contribution from a Fellow of the American Academy of Microbiology.

Hepatitis C virus (HCV) infects 200 million people worldwide and is the most prevalent viral pathogen for which there is no vaccine (1). HCV is a positive-stranded, enveloped RNA virus of approximately 9.6 kb in length, with 5' and 3' untranslated regions and one long open reading frame encoding a single polyprotein (1). The virus genome replicates by an RNA-dependent RNA polymerase and is notable for its extensive diversity within and among individuals; globally, there are seven major HCV genotypes that differ by approximately 30% at the nucleotide level (2). The different HCV genotypes exhibit variable responsiveness to interferon (IFN)-based and the newer direct-acting antiviral ther-

apies (3); moreover, HCV heterogeneity complicates studies of viral tropism and pathogenesis, and it is a major obstacle to development of effective vaccines (2). In this regard, the acute infection period is associated with the lowest viral diversity, theoretically making the early transmitted virus the most vulnerable to immune responses (2).

The precise determinants of immunity toward HCV are only partially characterized. HCV reaches the liver via the portal vein or the hepatic artery and infects hepatocytes, the known major site of replication (4). The liver is comprised of many different cell types that, despite not sustaining productive viral replication, are likely able to

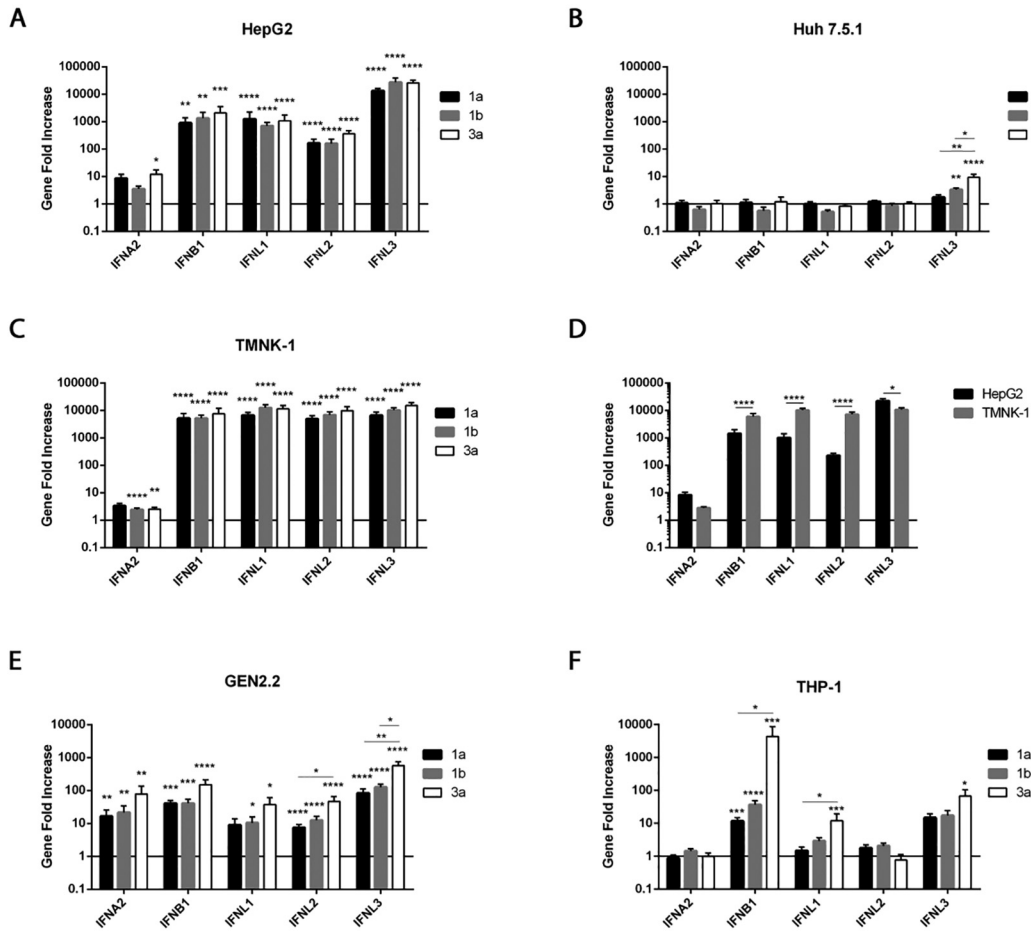


**FIG 1** HCV T/F vRNA transfected into liver cells induces IFN responses. IFN gene expression was determined by qRT-PCR in HepG2 (A), Huh 7.5.1 (B), TMNK-1 (C), GEN2.2 (E), and THP-1 (F) cells after 8 h of transfection with 1  $\mu$ g T/F vRNA. (D) Overall responses to T/F vRNA transfection were compared in HepG2 and TMNK-1 cells by combining and averaging the gene fold increase values across all genotypes from Fig. 1A or C, respectively. Gene fold increases were calculated relative to mock transfection. *P* values are results of Mann-Whitney comparisons of the bars indicated versus mock transfection (*n* = 3); those with lines below asterisks indicate Mann-Whitney comparisons of the 2 bars indicated. \*, *P* < 0.05; \*\*, *P* < 0.01; \*\*\*, *P* < 0.001; \*\*\*\*, *P* < 0.0001. Bars represent the mean, and error bars are  $\pm$  the standard error of the mean (SEM).

sense HCV RNA and shape the outcome of infection (5). Considering the abundant diversity of cells, we reasoned that the site of initial infection might play a critical role in regulation of HCV replication within hepatocytes. In other words, the lack of early, robust antiviral responses following intracellular HCV RNA sensing may be a harbinger of unchecked progression of the virus toward persistence.

Recent studies of HIV-1 transmission based on single-genome amplification (SGA), direct amplicon sequencing, phylogenetic inference, and mathematical modeling of early virus replication and diversification revealed a stringent population bottleneck with one or a few viruses generally leading to productive virus infection (6, 7). These studies showed that full-length replication-competent viral genomes could be identified and cloned, and interestingly, there was a suggestion that transmitted/founder (T/F) HIV-1 viruses would be preferentially resistant to interferon (7). More recently, the same single-genome sequencing (SGS) approach was used to identify and clone T/F HCV genomes (2, 8). Although cloned T/F HCV genomes by definition possess sequences that favor efficient *in vivo* replication in humans and are responsible for transmission and productive infection (2), their biological effects on different cell types, including those involved

in innate and adaptive immune responses, have not been characterized. The aim of the present study was to determine how HCV T/F genomes differentially activate antiviral IFN signaling. Due to the multiple parenchymal and nonparenchymal cell types that make up the liver, we used a comprehensive approach to study hepatocytes, liver endothelial cells, monocytes, and plasmacytoid dendritic cells (pDCs) transfected with genotype 1a, 1b, or 3a viral RNA (vRNA). The results provide novel insights into genotype-specific and cell-type-specific responses to early HCV infection and understanding of potential mechanisms of viral persistence.

**RESULTS**

**Differential induction of type I and III IFNs by hepatitis C T/F viral genomes in cell types comprising the liver.** As hepatocytes are the natural reservoir and primary site of replication for HCV, we started by transfecting two human hepatoma cell lines, HepG2 and Huh 7.5.1, with HCV T/F virus genotype 1a, 1b, and 3a vRNA. Robust transcriptional upregulation of IFNB1, interleukin-28A (IL-28A [IFNL2]), and IL-29 (IFNL1) were noted in HepG2 cells but not Huh 7.5.1 cells (Fig. 1A versus 1B) after 8 h, in keeping with the defective IFN signaling in the latter cells. In this regard,

## 8 Hour Transfection

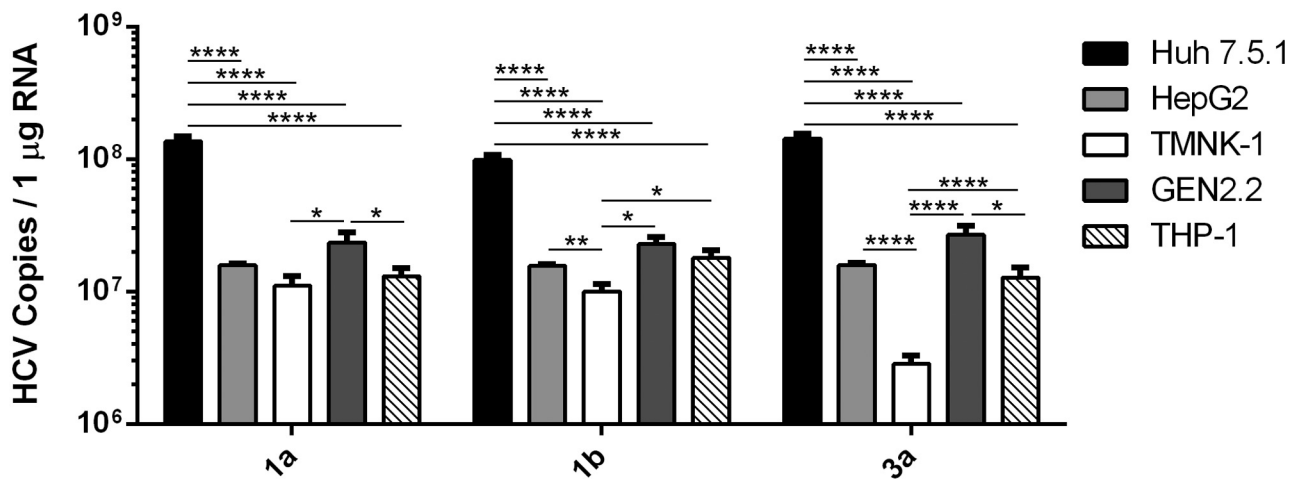


FIG 2 HCV T/F vRNA is degraded in HepG2, TMNK-1, GEN2.2, and THP-1 cells. Shown is the HCV copy number in all cell types as determined by qRT-PCR after 8 h of transfection with 1 µg T/F vRNA (genotype 1a, 1b, or 3a). Mann-Whitney comparisons of the 2 bars indicated are presented. \*,  $P < 0.05$ ; \*\*,  $P < 0.01$ ; \*\*\*,  $P < 0.001$ ; \*\*\*\*,  $P < 0.0001$ . Bars represent the mean, and error bars are  $\pm$  SEM.

both the presence of a single dominant-negative point mutation in the dsRNA sensor retinoic acid-inducible gene I (RIG-I) and lack of Toll-like receptor 3 (TLR3) expression within Huh 7.5.1 cells are critical for the higher permissiveness for HCV replication (50-fold greater than reported previously in other cells) (9, 10). Therefore, the comparatively lower IFN gene transcription in these cells is not unexpected.

Liver endothelial cells compose the highest proportion (approximately 50%) of the nonparenchymal cells and are highly efficient scavengers that pinocytose particles that are  $<0.2$  µm, such as virus-sized particles (11). The recent demonstration that liver sinusoidal endothelial cells (LSECs) and not Kupffer cells clear the bulk of blood-borne human adenovirus underscores their potential importance during the viremic phase of any natural viral infection (11). Transfection of the immortalized, differentiated adult human liver endothelial cell line TMNK-1 (12) with HCV T/F vRNA (compared to mock transfection) induced even greater upregulation of IFNB1 ( $P < 0.0001$ ), IFNL1 ( $P < 0.0001$ ), and IFNL2 ( $P < 0.0001$ ) than that noted for HepG2 cells (Fig. 1C and D). Notably, IFNL3 was induced at a statistically higher level within HepG2 cells ( $P = 0.0138$ ). Furthermore, the HCV genotype did not appear to affect the patterns of IFN responses within HepG2 or TMNK-1 cells.

Plasmacytoid dendritic cells (pDCs) play a critical role as innate pathogen sensors (13). Although they constitute only 0.2% to 0.8% of peripheral leukocytes in healthy subjects, pDCs have been found to produce over 95% of peripheral blood mononuclear cell (PBMC)-derived type I IFNs in response to many viruses (13). HCV-specific sequences have been detected in RNA extracts of DCs (4). Moreover, IFN production is mediated by TLR7 activation independently of HCV RNA replication (14), and the pathogen-associated molecular pattern (PAMP) [i.e., the HCV genome 3' nontranslated poly(U/UC) tract] signals through the cytosolic receptor RIG-I within pDCs (15). We found that transfection with HCV T/F vRNA induced high levels of type I and type III IFNs within a pDC line (GEN2.2) (15, 16), particularly with

HCV genotype 3a, which is associated with higher spontaneous recovery (17) and IFN treatment-induced response than either genotype 1a or 1b (18) (Fig. 1E).

Kupffer cells constitute the first macrophage population with which pathogens, bacterial endotoxins, and microbial debris from the gastrointestinal tract come in contact (46). Together with the liver sinusoidal endothelial cells (LSECs), these cells make up the hepatic reticuloendothelial system (20). Previously, it has been reported that HCV entered Kupffer cells via phagocytic uptake independently of productive infection, leading to induction of IFN- $\beta$ -dependent innate immune responses through the RIG-I and mitochondrial antiviral signaling (MAVS) pathways (5). In the present study, transfection of the monocyte cell line THP-1 with HCV T/F vRNA resulted in increased IFNB1 but no significant IFNA2 and relatively modest IFNL2 and IFNL3 transcription (Fig. 1F). Furthermore, as demonstrated for pDC, HCV T/F virus transfection with genotype 3a vRNA in THP-1 yielded higher IFN levels than either genotype 1a or 1b.

Importantly, the transfection efficiencies for the three different HCV T/F virus genomes were equivalent in all of the types tested (see Fig. S1 in the supplemental material). Therefore, differences in gene upregulation cannot be attributed to transfection efficiency of the vRNA. Additionally, transfection of an irrelevant RNA (pUC19) induced substantially lower IFN responses in all cell types (see Fig. S2 in the supplemental material). Furthermore, we found that T/F vRNA transfection into Huh 7.5.1 cells did not result in productive viral replication after 3, 5, or 7 days (see Fig. S3 in the supplemental material) (data not shown), indicating that the responses were not generated due to active viral replication. Interestingly, HCV copy number was significantly decreased in HepG2, TMNK-1, GEN2.2, and THP-1 cells 8 h posttransfection compared to Huh 7.5.1 cells, with TMNK-1 cells degrading the vRNA to the greatest extent (Fig. 2).

**Secretion of antiviral proteins after T/F vRNA transfection.** We next analyzed the ability of the different cells to produce and secrete IFN proteins after T/F vRNA transfection. IFN multiplex

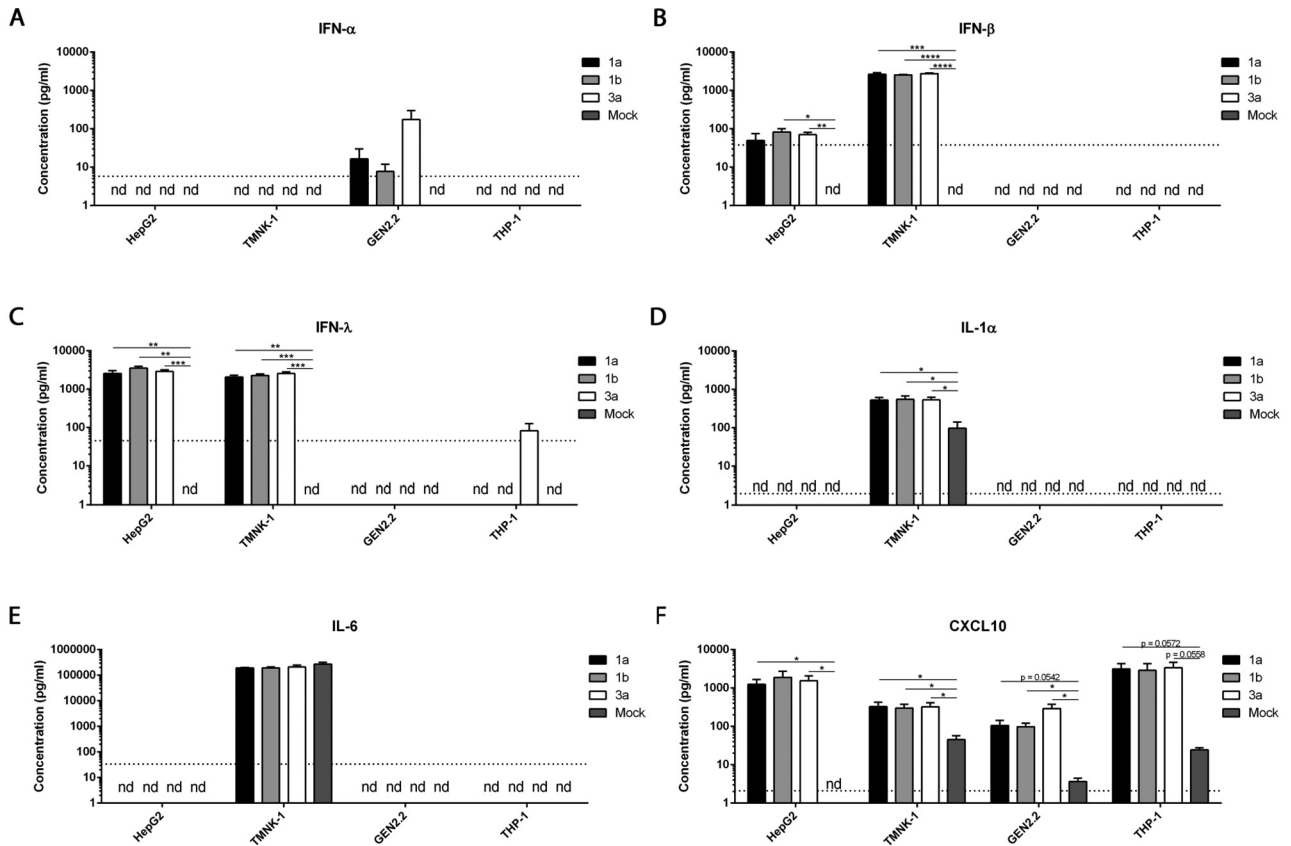


**FIG 3** Upregulation of IFN proteins after T/F vRNA transfection in hepatocytes, LSECs, pDCs, and monocytes. IFN protein production was determined by ELISA on supernatants collected from HepG2, TMNK-1, GEN2.2, and THP-1 cells after 24 h of transfection with 1  $\mu$ g T/F vRNA (genotype 1a, 1b, or 3a). Note the scale difference in panel E. *P* values are results from unpaired *t* tests of the bars indicated. \*, *P* < 0.05; \*\*, *P* < 0.01; \*\*\*, *P* < 0.001; \*\*\*\*, *P* < 0.0001. Bars represent the mean, and error bars are  $\pm$  SEM (*n* = 3). nd, not determined.

enzyme-linked immunosorbent assays (ELISAs) were performed on supernatants collected from HCV T/F vRNA-transfected cells at 24 h, and the concentrations of IFN- $\alpha$ , IFN- $\beta$ , IFN- $\lambda$ , IL-1 $\alpha$ , IL-6, and CXCL10 (C-X-C motif chemokine 10 [IP-10]) were measured (Fig. 3). In agreement with the data from Fig. 1 and 2, the GEN2.2 pDC was the only cell type to produce IFN- $\alpha$  protein (Fig. 3A), while TMNK-1 and HepG2 cells generated the highest levels of IFN- $\beta$  (Fig. 3B) and IFN- $\lambda$  (Fig. 3C) proteins. Additionally, TMNK-1 cells were the only cell type to produce IL-1 $\alpha$  (Fig. 3D) and IL-6 (Fig. 3E). Interestingly, mock-transfected TMNK-1 cell supernatants also displayed high levels of both IL-1 $\alpha$  and IL-6, suggesting that these cells may constitutively produce high levels of the proteins. Nonetheless, T/F vRNA transfection with all genotypes induced statistically larger amounts of IL-1 $\alpha$  secreted from TMNK-1 cells than mock transfection. In contrast, T/F vRNA transfection induced no additional effect on the production of IL-6 versus mock transfection in TMNK-1 cells. Finally, CXCL10 protein was generated from all cell types after T/F vRNA transfection (Fig. 3F), with the highest to lowest levels of production as follows: THP-1, HepG2, TMNK-1, and GEN2.2 cells. All cells secreted CXCL10 in response to mock transfection, except HepG2 cells, but most T/F vRNA transfection conditions were statistically higher than the respective mock conditions. We observed no genotype differences for any protein in the superna-

tants, as had been seen in GEN2.2 pDCs and THP-1 monocytes at the gene level (Fig. 1E and F).

**Supernatants derived from T/F-transfected hepatocytes and liver endothelial cells, but not monocytic or plasmacytoid DCs, inhibit HCV replication.** Given the intimate anatomic relationship between many of the cells types within the liver, we next sought to determine the ability of supernatants from cells transfected with HCV T/F vRNA to control HCV replication. Supernatants from T/F vRNA-transfected cells were collected and added simultaneously with JFH-1 infectious supernatant to Huh 7.5.1 cells. Three days later, the Huh 7.5.1 cells were evaluated for HCV copy number. As shown in Fig. 4, treatment with supernatants from both HepG2 cells and TMNK-1 cells resulted in significant inhibition of HCV replication compared to mock transfection, consistent with our data demonstrating higher IFN gene upregulation and protein production in those cell types. Supernatants from the GEN2.2 pDCs or THP-1 monocytes were unable to control viral replication, perhaps because of relatively lower secretion of antiviral proteins, as shown in Fig. 3.

**Uptake of exogenous T/F vRNA also induces IFN transcription in HepG2, THP-1, and TMNK-1 cells.** Because *in vitro* transfection of cells may induce a supraphysiologic response, we tested the ability of specific cell types to naturally take up and recognize HCV. As shown in Fig. S4 in the supplemental material, both



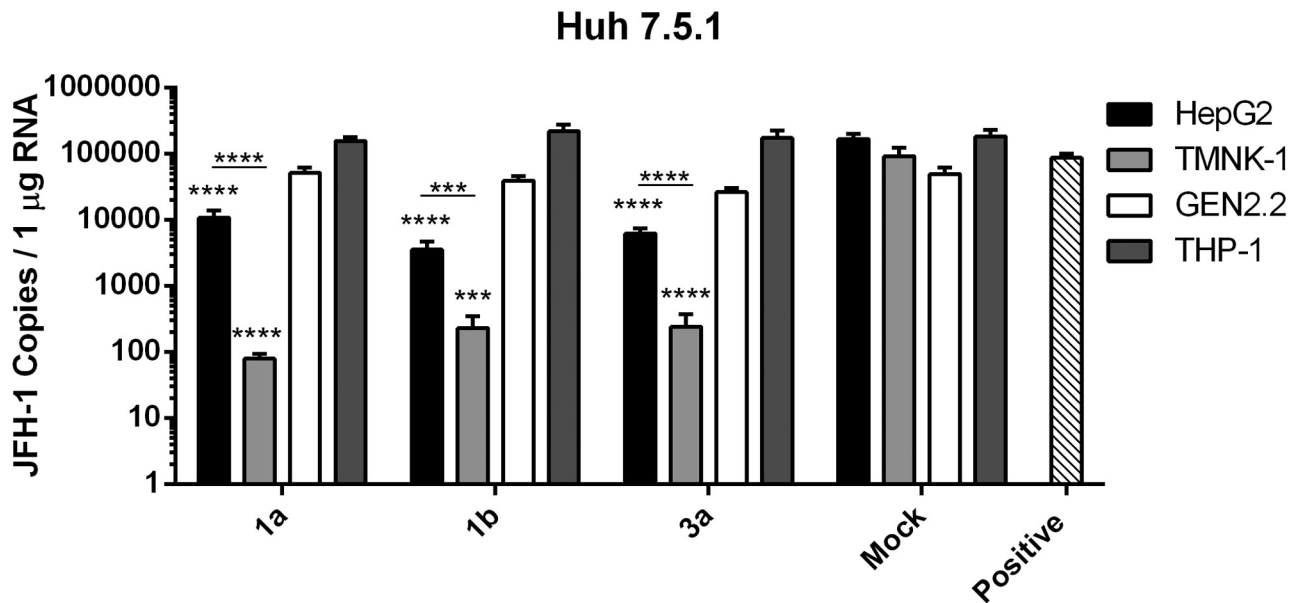


**FIG 4** Inhibition of viral replication by supernatants of T/F vRNA-transfected cells. Shown is the JFH-1 copy number determined by qRT-PCR in Huh 7.5.1 cells after 3 days of infection with JFH-1. Supernatants collected from 24-h-transfected (1 µg T/F vRNA, genotype 1a, 1b, or 3a) GEN2.2, THP-1, HepG2, or TMNK-1 cells were added to the Huh 7.5.1 cells simultaneously with JFH-1. Positive-control wells were infected with JFH-1 and given culture medium only. Negative-control wells were given culture medium only (not shown). Copy number was calculated based on a standard curve analysis. *P* values are results of Mann-Whitney comparisons of the bars indicated versus mock transfection. \*\*\*, *P* < 0.001; \*\*\*\*, *P* < 0.0001. Bars represent the mean, and error bars are ± SEM (*n* = 3 individual experiments).

HepG2 and THP-1 cells demonstrated upregulation of IFNs after addition of T/F vRNA directly to the media, although, as expected, to a less robust extent than following transfection. TMNK-1 cells were also able to take up exogenous T/F vRNA and upregulate type I and III IFNs (21).

**T/F vRNA transfection in primary human cells.** While the use of multiple immortalized cell lines can provide important insights, they have several limitations with regard to faithfully replicating human immunopathology. Accordingly, we next investigated the effect of transfecting T/F vRNA into functionally stable primary human hepatocyte (PHH) cells maintained as micropatterned cocultures, as described previously (22). As shown in Fig. 5A, transfection of primary human hepatocyte cells for 8 h resulted in robust upregulation of IFN genes, although in general, to a lower extent than observed with HepG2 cells. Similarly to most other cell types, PHH cells did not express IFNA2 in response to T/F vRNA transfection. Interestingly, these hepatocytes responded differentially according to genotype, with 3a inducing significantly higher levels of most genes. In contrast, the two hepatocyte cell lines we had analyzed did not display differences among genotypes (Fig. 1).

Additionally, we transfected primary human macrophages that were isolated by CD14<sup>+</sup> magnetic bead separation from whole PBMCs and further differentiated using macrophage colony-stimulating factor (M-CSF). IFN gene upregulation was similar in pattern to what was seen in THP-1 cells (Fig. 5C versus Fig. 1F). As was seen in THP-1 cells, differentiated macrophages displayed a genotype-specific response in that some IFN genes were upregulated to a greater extent after transfection with genotype 3a versus 1a.

In order to more comprehensively assess gene expression patterns in an unbiased approach, we subjected PHH cell lysates after

8 h of transfection with either genotype 1a or 3a T/F vRNA to transcriptomic microarray analysis. Compared to mock transfection, hepatitis C vRNA induced nearly identical transcriptional responses for the majority of genes regardless of genotype (i.e., >99% identity between genotypes 1a and 3a) (Fig. 6A). The top biological network identified by the platform Ingenuity Pathway Analysis (IPA) as being altered after genotype 3a vRNA transfection in PHH is shown in Fig. 6B. Fisher's exact test was used to calculate the probability that the biological associations between these genes would be explained by chance alone ( $P < 10^{-27}$ ). This network included many chemokine (CXCL10 and CXCL11), type I and III IFN, and IFN-stimulated genes. Significant differences in gene expression of CXCL10, CXCL11, EGR1 (early growth response protein 1), and IFIT3 (interferon-induced protein with tetratricopeptide repeats 3) observed in genotype 3a- versus 1a-transfected PHH cells by microarray analysis were confirmed via qRT-PCR (Fig. 5B). The microarray analysis had predicted a higher induction of HIST1H3F (histone cluster 1, H3f) in genotype 1a versus 3a; however, this was not confirmed by quantitative reverse transcription-PCR (qRT-PCR) (Fig. 5B).

IPA identified RIG-I (DDX58), which serves as a cytoplasmic sensor for HCV (1), and STAT1 target genes as being overrepresented in the PHH transcripts from cells transfected with genotype 3a vRNA compared to genotype 1a vRNA (Fig. 6C). IPA analysis predicted that STAT1 is upregulated to a greater extent in genotype 3a-transfected cells, and EGR1 expression has been shown to be increased in a STAT1 homozygous knockout mutant in mice (23). However, EGR1 was found to be upregulated via microarray analysis and confirmatory qRT-PCR. This inconsistency could be due to dysregulation of signaling in the pathway between STAT1 and EGR1. The dysregulation may lead to an apparent discrepancy where both genes may be upregulated, but the STAT1 inhib-

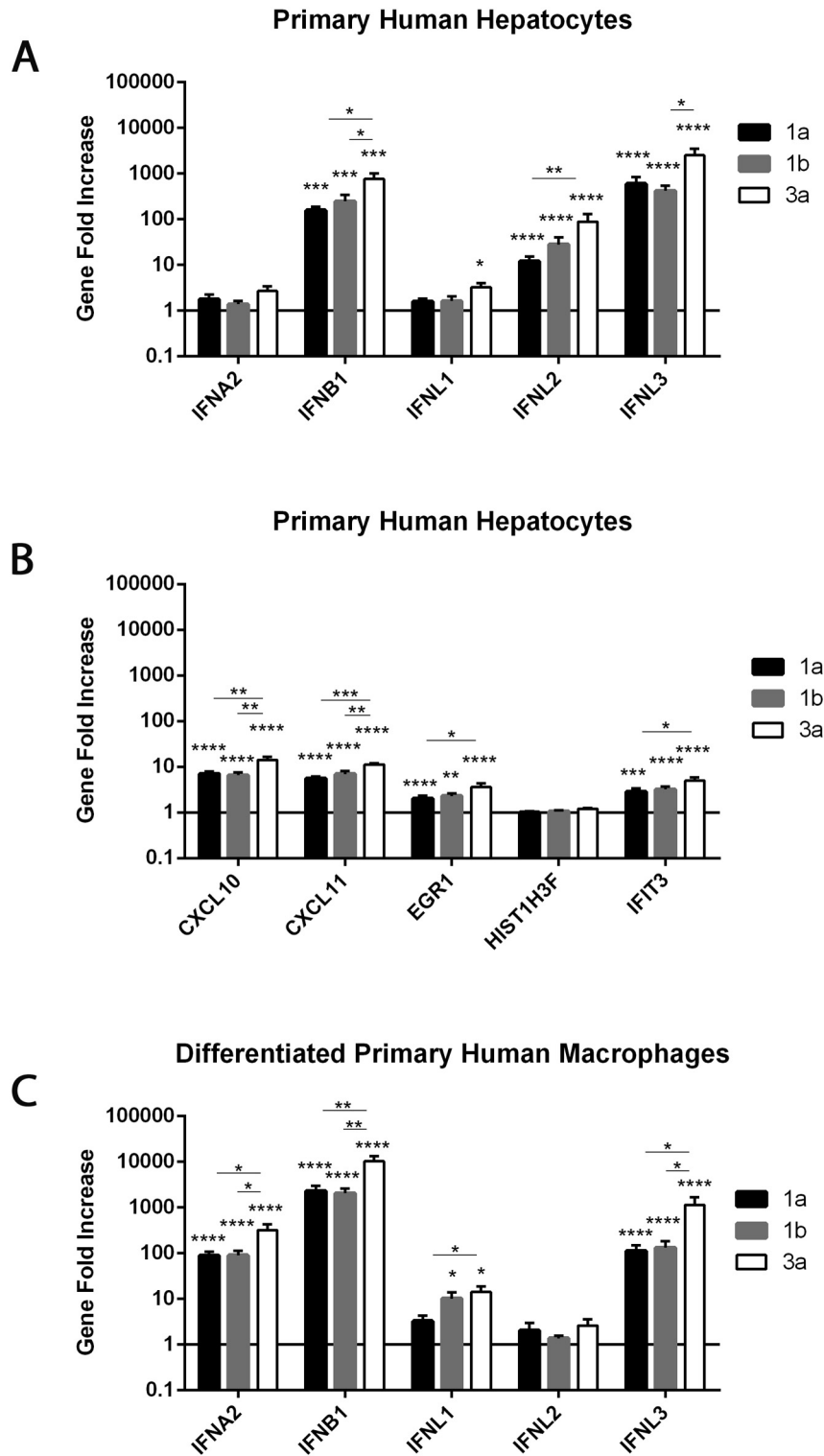


**FIG 5** HCV T/F vRNA transfection into primary human cells induces an upregulation of gene expression. (A) IFN gene expression determined by qRT-PCR in PHH cells after 8 h of transfection with 1  $\mu$ g T/F vRNA. (B) Microarray follow-up qRT-PCR analysis of PHH cells after 8 h of transfection with 1  $\mu$ g T/F vRNA. (C) IFN gene expression determined by qRT-PCR in differentiated human macrophages after 8 h of transfection with 1  $\mu$ g T/F vRNA. Gene fold increases were calculated relative to mock transfection. *P* values are results from Mann-Whitney comparisons of the bars indicated versus mock transfection; those with lines below asterisks indicate Mann-Whitney comparisons of the 2 bars indicated. \*, *P* < 0.05; \*\*, *P* < 0.01; \*\*\*, *P* < 0.001; \*\*\*\*, *P* < 0.0001. Bars represent the mean, and error bars are  $\pm$  SEM. *n* = 3 for qRT-PCR analyses (unpooled cellular RNA); shown is pooled cellular RNA from *n* = 3 independent experiments for each microarray slide.

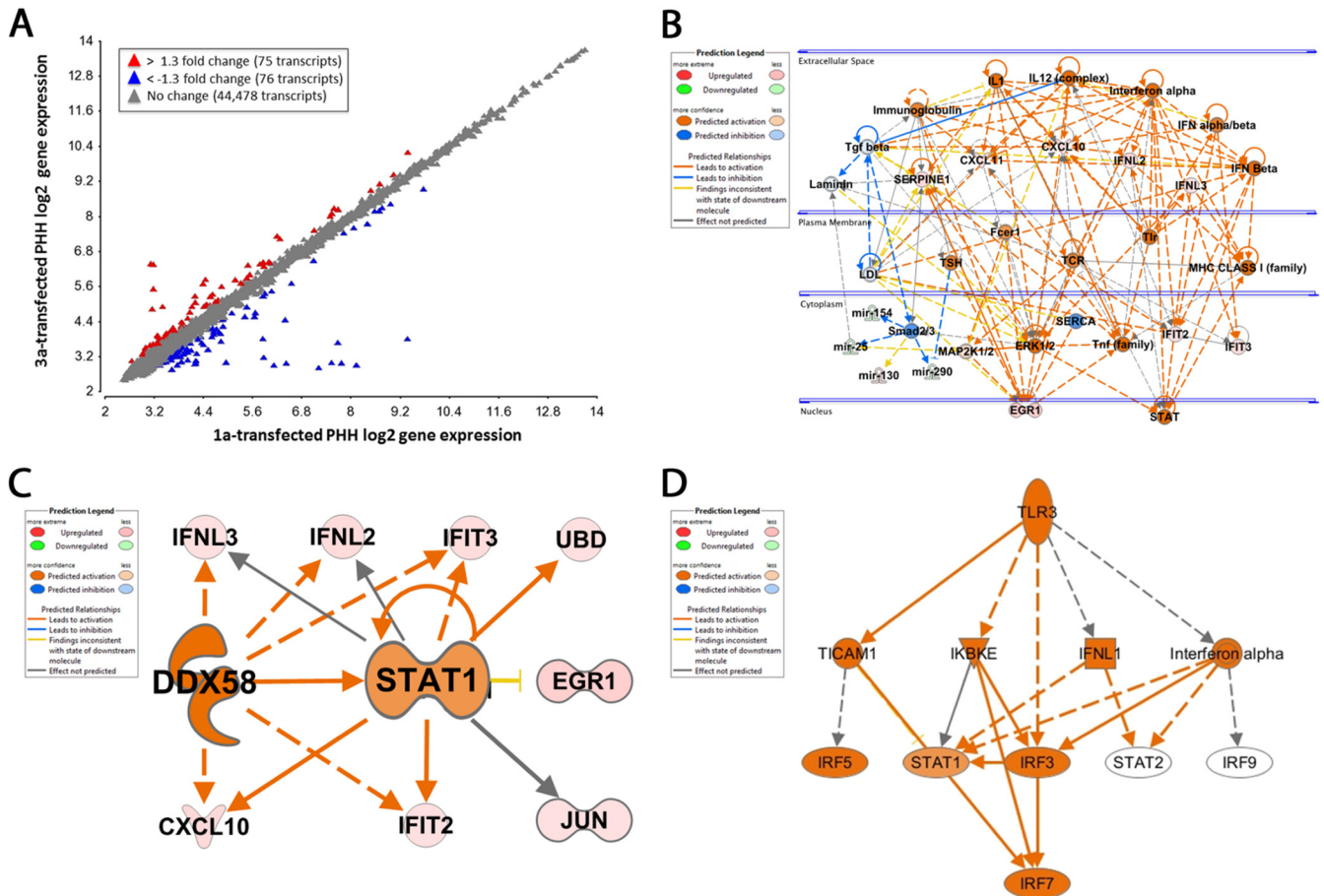


**FIG 6** PHHs respond to genotype 3a T/F vRNA via upregulation of the RIG-I, STAT1, and TLR3 pathways. (A) Scatter plot of log<sub>2</sub> gene expression of pooled cellular RNA from primary human hepatocytes (PHHs) transfected with genotype 1a (x axis) versus 3a (y axis) T/F vRNA ( $n = 3$ ). An absolute fold change cutoff of greater than 1.3 was used to identify a list of 151 out of a total of 44,629 measured transcripts different between the responses to the two HCV genotypes. (B) Top IPA biological network produced from genes altered in the 3a T/F vRNA response. The network was created on the Ingenuity Pathway Analysis (IPA) platform, utilizing the 60 out of 151 transcripts different ( $|\text{fold change}| > 1.3$ ) in the 3a versus 1a T/F vRNA response that had biological information available for systems analysis. The probability of getting the direct (solid lines) and indirect (dashed lines) biological relationships in our original list of transcripts due to random chance is  $\sim 10^{-27}$  (Fisher's exact test). (C) DDX58 and STAT1 target genes are overrepresented in transcripts upregulated in PHH response to 3a versus 1a T/F vRNA. The probabilities of getting the 5 downstream targets of DDX58 and the 8 targets of STAT1 by random chance in our gene list are  $2 \times 10^{-8}$  and  $3 \times 10^{-10}$ , respectively (Fisher's exact test). (D) TLR3 upstream network. All genes in this network have potential downstream targets overrepresented in the transcripts differentially expressed in the PHH 3a versus 1a T/F vRNA response, with a pattern of expression of these target genes suggesting increased activation in the 3a response for those members colored in orange.

itory effects on EGR1 are not realized. However, with the exception of EGR1, several target genes associated with STAT1 and RIG-I were consistent with our qRT-PCR data (IFNL2, IFNL3, IFIT3, and CXCL10). Additionally, IPA analysis identified a TLR3 network, which consists of potential genes (the IFN- $\alpha$ , IFN regulatory factor 3 [IRF3], IRF7, and STAT1 genes, for example) with overrepresented downstream targets after genotype 3a versus genotype 1a vRNA transfection (Fig. 6D).

## DISCUSSION

Multiple cell types with diverse properties, including antiviral and inflammatory potential, reside within sites of HCV entry and replication in the liver. Using novel hepatitis C transmitter/founder vRNA, shown in the accompanying article by Stoddard et al. (8) to represent viral products well suited for transmission and early replication, we compared the biological responses of these cells: specifically, the induction of IFNs known to play key roles in host

defense against viral infections. Of central relevance is the understanding that nonparenchymal cells (NPCs) do not require viral replication for direct recognition and subsequent IFN production (24). For the first time, we demonstrate that hepatitis C vRNA sensing triggers differential type I and III IFN responses across a wide variety of hepatic cells that may also vary according to HCV genotype. We show that liver endothelial cells, comprising the largest proportion of NPCs in the liver (11), demonstrated the highest transcription of IFN genes and, indeed, higher protein secretion of IFN- $\beta$  than HepG2 cells following transfection of equivalent amounts of HCV RNA (Fig. 3). Transfection of the immortalized, differentiated adult human liver endothelial cell line TMNK-1 (12) with HCV T/F vRNA (compared to mock transfection) induced greater upregulation of IFNB1 ( $P < 0.0001$ ), IFNL1 ( $P < 0.0001$ ), and IFNL2 ( $P < 0.0001$ ) than was noted for HepG2 cells (Fig. 1D). Interestingly, TMNK-1 cells demonstrated relatively greater HCV genome degradation (i.e.,

decrease in viral copy number [Fig. 2]); although the precise cellular pathways are unknown, one such mechanism may be microRNA (miRNA)-mediated degradation. Accordingly, in conjunction with induction of antiviral responses, IFN- $\beta$  has been shown to upregulate several cellular miRNAs with anti-HCV properties (25). Moreover, compared to more conventional immune cells (pDCs and monocytes), liver endothelial cells were remarkable in that their supernatants (following T/F vRNA transfection) were more potent in the control of HCV replication.

Recently, Negash and colleagues demonstrated that HCV enters Kupffer cells independently of productive infection, leading to induction of IFN- $\beta$ -dependent innate immune responses through RIG-I/MAVS (5). Expanding on those results, we found that transfection of the monocyte cell line THP-1 with the HCV T/F vRNA resulted in increased IFNB1 and IFN- $\lambda$  transcription. Moreover, in the monocyte and pDC lines and in macrophages differentiated from monocytes with MCSF, genotype 3a induced greater IFN transcription than either genotype 1a or 1b. These results potentially provide mechanistic insights into several important clinical observations. Acutely HCV-infected patients are much more likely to spontaneously clear HCV if infected with genotype 3 compared to genotype 1 (17). Patients chronically infected with genotype 3 have much higher sustained virologic response rates and shorter requisite duration of treatment with pegylated IFN/ribavirin therapy compared to chronic genotype 1 infection (26). In patients who fail to respond to antiviral therapy, there is a consistent association of enhanced immune responses that are insufficient to mediate viral clearance but sufficient to induce greater liver cell injury (i.e., increased hepatic necroinflammation) (27). In particular, in patients with non-genotype 1 infection, the presence of IFN alleles that reduce the chances of viral clearance may paradoxically slow the rate of fibrosis progression in the setting of viral persistence (28).

Recent data indicate that HCV genotype 3 is associated with increased rate of fibrosis progression compared to non-3 genotypes (29–31) and, epidemiologically, is an independent risk factor for end-stage liver disease and hepatocellular carcinoma (32–34). One could speculate that the significantly higher NPC transcription of IFN genes following intracellular sensing of genotype 3 versus genotype 1 HCV vRNA in our study may account for some of these observations. Moreover, the analyses of transcriptional responses in PHH further support the mechanistic basis for these concepts because genotype 3a induced overrepresentation of the complementary pathogen recognition receptor (PRR) pathways, RIG-I and TLR3. RIG-I is critical for sensing intracellular viral RNA PAMPs, whereas TLR3 recognizes extracellular double-stranded RNA (dsRNA) generated from virus released from infected cells (1). A single-point mutation in RIG-I and the lack of TLR3 expression in the human hepatocellular carcinoma-derived cell line Huh 7.5.1 and its derivatives contribute to the greater permissiveness for HCV replication (9, 10), and the relative expression of these PRRs may explain the differences between the primary hepatocytes and the hepatocyte cell line described in the present study. Transfection of genotype 3a vRNA into PHHs, the major site of HCV replication, induced higher relative expression of IFNB1, IFNL2, and IFNL3, and hence, collectively, a more vigorous antiviral response. Microarray and confirmatory PCR identified other genes that were induced to a greater extent following genotype 3a sensing, including the gene coding for IFIT3, which is a member of an IFN-induced effector protein family that

contributes to viral inhibition (35). The chemokines CXCL10 and CXCL11 play important roles in chemoattraction for monocytes/macrophages, T cells, NK cells, and dendritic cells contributing to hepatic necroinflammation (36). The longstanding observation that patients with HCV genotype 3 have higher rates of hepatic steatosis has led to the speculation that specific viral sequences may increase lipogenesis and inhibit fatty acid degradation (37). Our comprehensive transcriptional analyses in PHHs support an alternative explanation beyond putative metabolic differences induced by HCV genotype 3; instead, the induction of proinflammatory chemokines and subsequent recruitment of inflammatory cells to the liver might be the forerunner to steatosis. As a related precedent, it has been shown that depletion of Kupffer cells prevents the development of diet-induced hepatic steatosis (38). Finally, the higher induction of EGR1 related to genotype 3a is of interest in that it has been identified recently as a molecular marker for the development of hepatocellular carcinoma in patients with HCV-related cirrhosis (19); moreover, IPA predicted inhibition of miRNA-154 and miRNA-25, both recently linked with suppression of cancer cell growth (39–41).

In summary, this is the first study to examine the effects of HCV T/F vRNA on multiple cell types within the hepatic compartment. The results elucidate HCV genotype- and cell-type-specific responses and point to a model whereby the cellular localization of HCV and the viral genotype play important roles in determining IFN signaling and, ultimately, control of viral replication. These results represent an important advance in our understanding of how different HCV genotypes affect hepatic immunity and inflammation and may inform the design of new therapies.

## MATERIALS AND METHODS

**Cell culture.** The hepatoma cell lines HepG2 (ATCC) and Huh 7.5.1 (Francis Chisari, Scripps Research Institute, La Jolla, CA) were maintained in Dulbecco's modified Eagle's medium (DMEM) supplemented with 10% fetal bovine serum (FBS), 1 $\times$  nonessential amino acids (NEAA) (Life Technologies, Grand Island, NY), and 1% penicillin–streptomycin (Invitrogen, Carlsbad, CA).

The TMNK-1 immortalized liver endothelial cell line was provided by A. Soto-Gutierrez (University of Pittsburgh, Pittsburgh, PA). TMNK-1 cells were maintained in high-glucose DMEM modified with 10% fetal bovine serum (FBS) and 1% penicillin–streptomycin (Invitrogen).

The pDC cell line, GEN2.2 (7), was grown on the mouse stromal cell line MS-5 (DSMZ, Braunschweig, Germany) in RPMI medium (Invitrogen) with 10% FBS, 1 $\times$  NEAA (Life Technologies), 1 $\times$  sodium pyruvate (Invitrogen), and 1 $\times$  gentamicin (Invitrogen). MS-5 cells were grown to 90% confluence before GEN2.2 cells were added. The nonadherent (GEN2.2) fraction of the culture was utilized in all experiments.

The THP-1 acute monocytic leukemia cell line (ATCC) was maintained in RPMI medium (Invitrogen) with the addition of 10% FBS and 0.05 mM 2-mercaptoethanol (Sigma-Aldrich, St. Louis, MO).

Cryopreserved primary human hepatocytes were purchased from Triangle Research Laboratories (Research Triangle Park, NC). Cryopreserved hepatocyte vials were thawed at 37°C for 120 s, followed by dilution with 50 ml of prewarmed hepatocyte culture medium (HCM) as described previously (16). The cell suspension was spun at 50  $\times$  g for 5 min. The supernatant was discarded, cells were resuspended in HCM, and viability was assessed using trypan blue exclusion (typically 80 to 95%). Liver-derived nonparenchymal cells, as judged by their size (~10  $\mu$ m in diameter) and morphology (nonpolygonal), were consistently found to be less than 1% in these preparations. To create micropatterned cocultures in 24-well plates, a hepatocyte pattern was first produced by seeding hepatocytes on rat tail collagen (Corning Biosciences) type I-patterned



substrates that mediate selective cell adhesion (42). The cells were washed with medium 4 to 6 h later to remove unattached cells (leaving ~30,000 attached hepatocytes on 90 collagen-coated islands within each well of a 24-well plate) and incubated in HCM. 3T3-J2 murine embryonic fibroblasts (43) were seeded 18 to 24 h later to create cocultures. Culture medium was replaced every 2 days (~300  $\mu$ l per well of a 24-well plate). On day 7 of micropatterned cocultures, transfection for all conditions was carried out with T/F vRNA. A master mix for each transfection condition was made following manufacturer's protocol (*TransIT*-mRNA kit; Mirus, Madison, WI). Approximately 150  $\mu$ l of hepatocyte culture medium was removed from the cultures, and 100  $\mu$ l of master mix was added in triplicate for each condition and time point. At 8 h posttransfection, cultures were lysed for gene expression analysis using RLT lysis buffer (Qiagen, Valencia, CA) with 10  $\mu$ l  $\beta$ -mercaptoethanol added per ml of lysis buffer to stabilize RNA. The RNA was sent through QiaShredder homogenizing columns (Qiagen) and then stored at  $-80^{\circ}\text{C}$  prior to further analysis using qRT-PCR.

Human PBMCs were maintained in medium containing RPMI plus 10% human serum. Primary human hepatocyte donors were deceased; as such, no consent was obtained. However, approval for all studies utilizing human cells and cell lines was granted through the Colorado Multiple Institutional Review Board (COMIRB 06-0566: "Novel Aspects of Hepatic Innate and Adaptive Immunity to HCV Infection").

**T/F virus DNA plasmid and vRNA generation.** Full-length HCV T/F sequences were determined from acute infection plasma vRNA by single-genome sequencing, phylogenetic inference, and a mathematical model of random early virus diversification, as described previously (2, 8). Full-genome-length T/F genomic sequences were generated by single-genome amplification chemically synthesized in 4 to 5 fragments (Blue Heron, Inc.), and ligated into low-copy-number pBR322 plasmids under control of the T7 promoter, which was added to the 5' end of the HCV genome in five overlapping fragments, and these sequences were used to enable *in vitro* transcription. T/F clones include 9.6-kb full-length HCV genotypes 1a (pBR322.10025TF.UC1), 1b (pBR322.10051TF.UC1), and 3a (pBR322.9055TF.UC1), with sequences contributed to GenBank (with accession numbers listed in the accompanying article by Stoddard et al. [8]). This strategy was required in order to obtain faithful representations of the 5' and 3' termini of the HCV genomes.

**T/F virus DNA plasmid and vRNA generation.** T/F and pUC19 (Invitrogen) DNA plasmids were transformed into Max Efficiency Stb12 competent cells (Invitrogen), and bacteria were plated on Luria-Bertani (LB) agar plates supplemented with ampicillin and incubated overnight at  $30^{\circ}\text{C}$ . Single colonies were selected and grown overnight in LB broth at  $30^{\circ}\text{C}$  with 225-rpm shaking. Miniprep plasmid DNA isolation was performed via the PureYield Plasmid Miniprep system (Promega, Madison, WI), and plasmid sizes were verified on an agarose gel (Bio-Rad, Hercules, CA). Maxiprep of the DNA plasmids was performed (Qiagen, Valencia, CA), and the DNA sequence of each plasmid was verified via DNA sequencing (with the BigDye terminator methodology and ABI 3730xl genetic analyzers; both from Applied Biosystems, Foster City, CA) and alignment (Sequencher program 5.0; Gene Codes, Ann Arbor, MI). Plasmids were linearized via restriction enzyme digest (New England Biolabs, Ipswich, MA) and *in vitro* transcribed using the T7-Scribe Standard RNA IVT kit (Cell Script, Madison, WI).

**T/F virus transfection.** TMNK-1, HepG2, or Huh 7.5.1 cells were plated in 12-well plates at a concentration of  $0.5 \times 10^6$  cells/ml, and THP-1 cells or pDCs were plated in 24-well plates at a concentration of  $1.0 \times 10^6$  cells/ml per well and rested overnight. Primary human hepatocytes (3 donors) were cultured as described above. Primary human CD14<sup>+</sup> bead-isolated cells were plated at  $0.5 \times 10^6$  cells per well in 12-well plates. One microgram of founder virus vRNA or an equivalent volume of RNase-free water (control) was diluted in transfection medium together with transfection reagents, according to the manufacturer's instructions (*TransIT*-mRNA kit; Mirus, Madison, WI). The prepared mixture was added to the cells for 8 or 24 h at  $37^{\circ}\text{C}$  in 5%  $\text{CO}_2$ .

Cellular RNA was isolated using RNeasy minikit (Qiagen) and quantified using a NanoDrop microspectrometer. cDNA was transcribed from 1  $\mu$ g of RNA using the QuantiTect RT kit (Qiagen). qRT-PCR was performed using SYBR green primers and master mix (Qiagen) and run on a StepOnePlus qPCR machine (Applied Biosystems). Data were analyzed using the threshold cycle ( $\Delta\Delta C_T$ ) method.

**T/F virus copy number and replication analysis.** For T/F virus copy number assays, qRT-PCR was performed using general HCV primers (HCV Forward, 5'-CGACACTCGCCATGAATCACT-3', and HCV Reverse 5'-CACTCGCAAGCGCCCTATCA-3') and TaqMan 6-carboxymethylrhodamine (TAMRA) probe (5'-6-carboxyfluorescein [6FAM]-AGGCCTTTCGCAACCAACGCTACT-TAMRA-3'). T/F virus copy number was determined using a standard curve.

For immunofluorescence staining, Huh 7.5.1 cells were transfected with T/F virus vRNA (1  $\mu$ g) for 3 days, fixed in 4% paraformaldehyde (PFA) for 30 min, and grown on coverslips overnight. Coverslips were adhered to microscope slides, were allowed to dry at room temperature in the dark, and then were blocked with 3% normal goat serum (Jackson ImmunoResearch, West Grove, PA). Primary antibody staining was performed using mouse anti-HCV Core (Thermo Scientific MAB1-080), and secondary antibody staining was via goat anti-mouse conjugated to Alexa Fluor 488 (Santa Cruz Biotechnology, Dallas, TX). Nuclei were stained with DAPI (4',6-diamidino-2-phenylindole). Slides were then mounted using ProLong Gold antifade reagent (Invitrogen), and images were captured at  $\times 40$  magnification using the EVOS FL Cell Imaging System (Invitrogen).

**ELISAs.** The Veriplex Human Interferon Multiplex ELISA kit was used for the ELISA, which was performed by PBL Interferon Service (Piscataway, NJ). All supernatants were harvested after 24 h of transfection with 1  $\mu$ g T/F virus vRNA and were used undiluted or at a 1:10 dilution in the assay.

**Viral control assays.** Huh 7.5.1 cells were plated at a concentration of  $0.125 \times 10^6$  cells/ml (1 ml) in a 24-well plate and incubated overnight. The following day, the medium was replaced with fresh medium, and the cells were infected with genotype 2a Japanese fulminate hepatitis strain 1 (JFH-1) (multiplicity of infection [MOI], 1.4). For viral infection assays (Fig. 4), supernatants collected from HepG2, GEN2.2, TMNK-1, or THP-1 cells transfected for 24 h with T/F virus vRNA (1  $\mu$ g) were added simultaneously with JFH-1 supernatants. Huh 7.5.1 cells were harvested for PCR 3 days postinfection. For viral control assays, Huh 7.5.1 cells were infected with JFH-1 for 5 days before supernatants from HepG2 or TMNK-1 cells transfected with T/F virus vRNA were added. Huh 7.5.1 cells were harvested for qPCR 24 h later. In both experiments, JFH-1 copy number was assessed in the Huh 7.5.1 cells via qRT-PCR using general HCV primers, as described above. JFH-1 copy number was determined using a standard curve. Positive-control wells were infected with JFH-1 and had no supernatants added. Negative-control wells were given culture medium only.

**Monocyte isolation and macrophage differentiation.** Whole human PBMCs were subjected to CD14<sup>+</sup> bead isolation (Miltenyi Biotec), as per the manufacturer's instructions. Purity was confirmed by flow cytometry. Macrophages were differentiated by the addition of 50 ng/ml M-CSF (PeproTech, Rocky Hill, NJ) for 7 days before vRNA transfection.

**Microarray and bioinformatics.** The pooled cellular RNAs from three independent PHH transfections (mock, 1a, or 3a T/F vRNA) were hybridized to Human Gene 2.0 Arrays (<http://www.affymetrix.com>) using standard Affymetrix protocols and converted to  $\log_2$  expression values, with RMA background correction adjusting for GC content and quantile normalization (44), as implemented by the statistical/visualization package Partek Genomics Suite v6.6 (<http://www.partek.com>). An absolute fold change cutoff of greater than 1.3 was used to identify transcripts different between the 3a versus 1a T/F vRNA response, yielding 151 out of a total of 44,629 transcripts measured on the array for subsequent bioinformatic analysis.

The platform Ingenuity Pathway Analysis (IPA) (<http://www.ingenuity.com>) was used to perform the systems analysis on the 60 out of 151

genes/miRNAs with available data for bioinformatic interpretation different in the transcriptional response of PHH cells to genotype 3a T/F vRNA. IPA uses a Fisher's exact test to identify overrepresented connected biological units in a defined set of genes, which can include pathways, cellular functions, or known targets of regulatory genes. In some cases, a confidence score, or Z score, can be made on the activation state of the pathway or upstream regulator based on the expression pattern of the associated genes (45). IPA was also used to group these transcripts into gene-limited networks (35 genes maximum) based on evidence of direct or indirect relationships between molecules according to the IPA Knowledge Base.

The IPA network algorithm seeks to maximize the interconnectivity within a group of selected genes and scores networks based on a right-tailed Fisher's exact test that calculates the probability that the given relationships can be explained by a random model. The constructed networks do not include all possible relationships for each member, due to size constraints placed on the network, and specific genes may appear in multiple networks.

**Statistical analyses.** Statistics were calculated using GraphPad Prism 6 software. Either Mann-Whitney tests (nonparametric) or unpaired *t* tests (two tailed) were utilized for comparisons between treated conditions and for fold increases of stimulated versus control conditions. Statistical significance was defined as  $P < 0.05$ .

**Microarray data accession number.** The normalized expression values used in the statistical and bioinformatics analysis for this article, as well as the original raw visual data used to calculate these values, have been deposited in the publicly accessible database Gene Expression Omnibus (<http://www.ncbi.nlm.nih.gov/geo/>) under accession no. GSE64400.

## SUPPLEMENTAL MATERIAL

Supplemental material for this article may be found at <http://mbio.asm.org/lookup/suppl/doi:10.1128/mBio.02510-14/-/DCSupplemental>.

Figure S1, PDF file, 0.1 MB.

Figure S2, PDF file, 0.1 MB.

Figure S3, PDF file, 2.7 MB.

Figure S4, PDF file, 0.1 MB.

Table S1, DOCX file, 0.01 MB.

## ACKNOWLEDGMENTS

This work was supported by R21 AI 103361 (National Institutes of Health), U19 AI 1066328 (HCV Center grant), and a VA Merit Review grant (Department of Veteran's Affairs) to H.R.R. and R21-AI 106000 (National Institutes of Health) to G.M.S.

## REFERENCES

- Rosen HR. 2013. Emerging concepts in immunity to hepatitis C virus infection. *J Clin Invest* 123:4121–4130. <http://dx.doi.org/10.1172/JCI67714>.
- Li H, Stoddard MB, Wang S, Blair LM, Giorgi EE, Parrish EH, Learn GH, Hrabec P, Goepfert PA, Saag MS, Denny TN, Haynes BF, Hahn BH, Ribeiro RM, Perelson AS, Korber BT, Bhattacharya T, Shaw GM. 2012. Elucidation of hepatitis C virus transmission and early diversification by single genome sequencing. *PLoS Pathog* 8:e1002880. <http://dx.doi.org/10.1371/journal.ppat.1002880>.
- Au JS, Pockros PJ. 2014. Novel therapeutic approaches for hepatitis C. *Clin Pharmacol Ther* 95:78–88. <http://dx.doi.org/10.1038/clpt.2013.206>.
- Racanelli V, Manigold T. 2007. Presentation of HCV antigens to naive CD8+T cells: why the where, when, what and how are important for virus control and infection outcome. *Clin Immunol* 124:5–12. <http://dx.doi.org/10.1016/j.clim.2007.04.009>.
- Negash AA, Ramos HJ, Crochet N, Lau DT, Doehle B, Papic N, Delker DA, Jo J, Bertoletti A, Hagedorn CH, Gale M, Jr. 2013. IL-1beta production through the nlrp3 inflammasome by hepatic macrophages links hepatitis C virus infection with liver inflammation and disease. *PLoS Pathog* 9:e1003330. <http://dx.doi.org/10.1371/journal.ppat.1003330>.
- Keele BF, Giorgi EE, Salazar-Gonzalez JF, Decker JM, Pham KT, Salazar MG, Sun C, Grayson T, Wang S, Li H, Wei X, Jiang C, Kirchherr JL, Gao F, Anderson JA, Ping LH, Swanstrom R, Tomaras GD, Blattner WA, Goepfert PA, Kilby JM, Saag MS, Delwart EL, Busch MP, Cohen MS, Montefiori DC, Haynes BF, Gaschen B, Athreya GS, Lee HY, Wood N, Seoighe C, Perelson AS, Bhattacharya T, Korber BT, Hahn BH, Shaw GM. 2008. Identification and characterization of transmitted and early founder virus envelopes in primary HIV-1 infection. *Proc Natl Acad Sci U S A* 105:7552–7557. <http://dx.doi.org/10.1073/pnas.0802203105>.
- Parrish NF, Gao F, Li H, Giorgi EE, Barbian HJ, Parrish EH, Zajic L, Iyer SS, Decker JM, Kumar A, Hora B, Berg A, Cai F, Hopper J, Denny TN, Ding H, Ochsenbauer C, Kappes JC, Galimidi RP, West AP, Jr, Bjorkman PJ, Wilen CB, Doms RW, O'Brien M, Bhardwaj N, Borrow P, Haynes BF, Muldoon M, Theiler JP, Korber B, Shaw GM, Hahn BH. 2013. Phenotypic properties of transmitted founder HIV-1. *Proc Natl Acad Sci U S A* 110:6626–6633. <http://dx.doi.org/10.1073/pnas.1304288110>.
- Stoddard MB, Li H, Wang S, Saeed M, Andrus L, Ding W, Jiang X, Learn GH, von Schaeuwen M, Wen J, Goepfert PA, Hahn BH, Ploss A, Rice CM, Shaw GM. 2015. Identification, molecular cloning, and analysis of full-length hepatitis C virus transmitted/founder genotypes 1, 3, and 4. *mBio* 6(1):e02518-14. <http://dx.doi.org/10.1128/mBio.02518-14>.
- Bartenschlager R, Pietschmann T. 2005. Efficient hepatitis C virus cell culture system: what a difference the host cell makes. *Proc Natl Acad Sci U S A* 102:9739–9740. <http://dx.doi.org/10.1073/pnas.0504296102>.
- Li K, Foy E, Ferreon JC, Nakamura M, Ferreon AC, Ikeda M, Ray SC, Gale M, Jr, Lemon SM. 2005. Immune evasion by hepatitis C virus NS3/4A protease-mediated cleavage of the Toll-like receptor 3 adaptor protein TRIF. *Proc Natl Acad Sci U S A* 102:2992–2997. <http://dx.doi.org/10.1073/pnas.0408824102>.
- Ganesan LP, Mohanty S, Kim J, Clark KR, Robinson JM, Anderson CL. 2011. Rapid and efficient clearance of blood-borne virus by liver sinusoidal endothelium. *PLoS Pathog* 7:e1002281. <http://dx.doi.org/10.1371/journal.ppat.1002281>.
- Matsumura T, Takesue M, Westerman KA, Okitsu T, Sakaguchi M, Fukazawa T, Totsugawa T, Noguchi H, Yamamoto S, Stolz DB, Tanaka N, Leboulch P, Kobayashi N. 2004. Establishment of an immortalized human-liver endothelial cell line with SV40T and hTERT. *Transplant* 77:1357–1365. <http://dx.doi.org/10.1097/01.TP.0000124286.82961.7E>.
- Lande R, Gilliet M. 2010. Plasmacytoid dendritic cells: key players in the initiation and regulation of immune responses. *Ann N Y Acad Sci* 1183:89–103. <http://dx.doi.org/10.1111/j.1749-6632.2009.05152.x>.
- Takahashi K, Asabe S, Wieland S, Garaigorta U, Gastaminza P, Isogawa M, Chisari FV. 2010. Plasmacytoid dendritic cells sense hepatitis C virus-infected cells, produce interferon, and inhibit infection. *Proc Natl Acad Sci U S A* 107:7431–7436. <http://dx.doi.org/10.1073/pnas.1002301107>.
- Stone AE, Giugliano S, Schnell G, Cheng L, Leahy KF, Golden-Mason L, Gale M, Jr, Rosen HR. 2013. Hepatitis C virus pathogen associated molecular pattern (PAMP) triggers production of lambda-interferons by human plasmacytoid dendritic cells. *PLoS Pathog* 9:e1003316. <http://dx.doi.org/10.1371/journal.ppat.1003316>.
- Chaperot L, Blum A, Manches O, Lui G, Angel J, Molens JP, Plumas J. 2006. Virus or TLR agonists induce TRAIL-mediated cytotoxic activity of plasmacytoid dendritic cells. *J Immunol* 176:248–255. <http://dx.doi.org/10.4049/jimmunol.176.1.248>.
- Lehmann M, Meyer MF, Monazahian M, Tillmann HL, Manns MP, Wedemeyer H. 2004. High rate of spontaneous clearance of acute hepatitis C virus genotype 3 infection. *J Med Virol* 73:387–391. <http://dx.doi.org/10.1002/jmv.20103>.
- Pol S, Vallet-Pichard A, Corouge M. 2014. Treatment of hepatitis C virus genotype 3-infection. *Liver Int* 34(Suppl 1):18–23. <http://dx.doi.org/10.1111/liv.12405>.
- Archer KJ, Mas VR, David K, Maluf DG, Bornstein K, Fisher RA. 2009. Identifying genes for establishing a multigenic test for hepatocellular carcinoma surveillance in hepatitis C virus-positive cirrhotic patients. *Cancer Epidemiol Biomarkers Prev* 18:2929–2932. <http://dx.doi.org/10.1158/1055-9965.EPI-09-0767>.
- Vollmar B, Menger MD. 2009. The hepatic microcirculation: mechanistic contributions and therapeutic targets in liver injury and repair. *Physiol Rev* 89:1269–1339. <http://dx.doi.org/10.1152/physrev.00027.2008>.
- Giugliano S, Kriss M, Golden-Mason L, Dobrinskikh E, Stone AE, Soto-Gutierrez A, Mitchell A, Khetani SR, Yamane D, Stoddard M, Li H, Shaw GM, Edwards MG, Lemon SM, Gale M, Jr, Shah VH, Rosen HR. 4 November 2014. Hepatitis C virus infection induces autocrine interferon signaling by human liver endothelial cell and release of exo-

- somes, which inhibits viral replication. *Gastroenterology* <http://dx.doi.org/10.1053/j.gastro.2014.10.040>.
22. Khetani SR, Kanchagar C, Ukairo O, Krzyzewski S, Moore A, Shi J, Aoyama S, Aleo M, Will Y. 2013. Use of micropatterned cocultures to detect compounds that cause drug-induced liver injury in humans. *Toxicol Sci* 132:107–117. <http://dx.doi.org/10.1093/toxsci/kfs326>.
  23. Ingram JL, Antao-Menezes A, Mangum JB, Lyght O, Lee PJ, Elias JA, Bonner JC. 2006. Opposing actions of Stat1 and Stat6 on IL-13-induced up-regulation of early growth response-1 and platelet-derived growth factor ligands in pulmonary fibroblasts. *J Immunol* 177:4141–4148. <http://dx.doi.org/10.4049/jimmunol.177.6.4141>.
  24. Kumagai Y, Kumar H, Koyama S, Kawai T, Takeuchi O, Akira S. 2009. Cutting edge: TLR-dependent viral recognition along with type I IFN positive feedback signaling masks the requirement of viral replication for IFN- $\alpha$  production in plasmacytoid dendritic cells. *J Immunol* 182:3960–3964. <http://dx.doi.org/10.4049/jimmunol.0804315>.
  25. Pedersen IM, Cheng G, Wieland S, Volinia S, Croce CM, Chisari FV, David M. 2007. Interferon modulation of cellular microRNAs as an antiviral mechanism. *Nature* 449:919–922. <http://dx.doi.org/10.1038/nature06205>.
  26. Hadziyannis SJ, Sette H, Jr, Morgan TR, Balan V, Diago M, Marcellin P, Ramadori G, Bodenheimer H, Jr, Bernstein D, Rizzetto M, Zeuzem S, Pockros PJ, Lin A, Ackrill AM, PEGASYS International Study Group. 2004. Peginterferon-alpha2a and ribavirin combination therapy in chronic hepatitis C: a randomized study of treatment duration and ribavirin dose. *Ann Intern Med* 140:346–355. <http://dx.doi.org/10.7326/0003-4819-140-5-200403020-00010>.
  27. Noureddin M, Wright EC, Alter HJ, Clark S, Thomas E, Chen R, Zhao X, Conry-Cantilena C, Kleiner DE, Liang TJ, Ghany MG. 2013. Association of IL28B genotype with fibrosis progression and clinical outcomes in patients with chronic hepatitis C: a longitudinal analysis. *Hepatology* 58:1548–1557. <http://dx.doi.org/10.1002/hep.26506>.
  28. Bochud PY, Bibert S, Kutalik Z, Patin E, Guergnon J, Nalpas B, Goossens N, Kuske L, Müllhaupt B, Gerlach T, Heim MH, Moradpour D, Cerny A, Malinverni R, Regenass S, Dollenmaier G, Hirsch H, Martinetti G, Gorgiewski M, Bourlière M, Poynard T, Theodorou I, Abel L, Pol S, Dufour JF, Negro F, Swiss Hepatitis C Cohort Study Group, ANRS HC EP 26 Genoscan Study Group. 2012. IL28B alleles associated with poor hepatitis C virus (HCV) clearance protect against inflammation and fibrosis in patients infected with non-1 HCV genotypes. *Hepatology* 55:384–394. <http://dx.doi.org/10.1002/hep.24678>.
  29. Bochud PY, Cai T, Overbeck K, Bochud M, Dufour JF, Müllhaupt B, Borovicka J, Heim M, Moradpour D, Cerny A, Malinverni R, Francioli P, Negro F, Swiss Hepatitis C Cohort Study Group. 2009. Genotype 3 is associated with accelerated fibrosis progression in chronic hepatitis C. *J Hepatol* 51:655–666. <http://dx.doi.org/10.1016/j.jhep.2009.05.016>.
  30. Goossens N, Negro F. 2014. Is genotype 3 of the hepatitis C virus the new villain? *Hepatology* 59:2403–2412. <http://dx.doi.org/10.1002/hep.26905>.
  31. Probst A, Dang T, Bochud M, Egger M, Negro F, Bochud PY. 2011. Role of hepatitis C virus genotype 3 in liver fibrosis progression—a systematic review and meta-analysis. *J Viral Hepat* 18:745–759. <http://dx.doi.org/10.1111/j.1365-2893.2011.01481.x>.
  32. Kanwal F, Kramer JR, Ilyas J, Duan Z, El-Serag HB. 2014. HCV genotype 3 is associated with an increased risk of cirrhosis and hepatocellular cancer in a national sample of U.S. veterans with HCV. *Hepatology* 60:98–105. <http://dx.doi.org/10.1002/hep.27095>.
  33. McMahon BJ, Bruden D, Bruce MG, Livingston S, Christensen C, Homan C, Hennessy TW, Williams J, Sullivan D, Rosen HR, Gretch D. 2010. Adverse outcomes in Alaska natives who recovered from or have chronic hepatitis C infection. *Gastroenterology* 138:922–931.e1. <http://dx.doi.org/10.1053/j.gastro.2009.10.056>.
  34. van der Meer AJ, Veldt BJ, Feld JJ, Wedemeyer H, Dufour JF, Lammert F, Duarte-Rojo A, Heathcote EJ, Manns MP, Kuske L, Zeuzem S, Hofmann WP, de Knegt RJ, Hansen BE, Janssen HL. 2012. Association between sustained virological response and all-cause mortality among patients with chronic hepatitis C and advanced hepatic fibrosis. *JAMA* 308:2584–2593. <http://dx.doi.org/10.1001/jama.2012.144878>.
  35. Metz P, Dazert E, Ruggieri A, Mazur J, Kaderali L, Kaul A, Zeuge U, Windisch MP, Trippler M, Lohmann V, Binder M, Frese M, Bartschlagler R. 2012. Identification of type I and type II interferon-induced effectors controlling hepatitis C virus replication. *Hepatology* 56:2082–2093. <http://dx.doi.org/10.1002/hep.25908>.
  36. Brass A, Brenndörfer ED. 2014. The role of chemokines in hepatitis C virus-mediated liver disease. *Int J Mol Sci* 15:4747–4779. <http://dx.doi.org/10.3390/ijms15034747>.
  37. Negro F. 2010. Hepatitis C virus-induced steatosis: an overview. *Dig Dis* 28:294–299. <http://dx.doi.org/10.1159/000282105>.
  38. Huang W, Metlakunta A, Dedousis N, Zhang P, Sipula I, Dube JJ, Scott DK, O'Doherty RM. 2010. Depletion of liver Kupffer cells prevents the development of diet-induced hepatic steatosis and insulin resistance. *Diabetes* 59:347–357. <http://dx.doi.org/10.2337/db09-0016>.
  39. Li Q, Zou C, Zou C, Han Z, Xiao H, Wei H, Wang W, Zhang L, Zhang X, Tang Q, Zhang C, Tao J, Wang X, Gao X. 2013. MicroRNA-25 functions as a potential tumor suppressor in colon cancer by targeting Smad7. *Cancer Lett* 335:168–174. <http://dx.doi.org/10.1016/j.canlet.2013.02.029>.
  40. Xin C, Zhang H, Liu Z. 2014. miR-154 suppresses colorectal cancer cell growth and motility by targeting TLR2. *Mol Cell Biochem* 387:271–277. <http://dx.doi.org/10.1007/s11010-013-1892-3>.
  41. Zhu C, Shao P, Bao M, Li P, Zhou H, Cai H, Cao Q, Tao L, Meng X, Ju X, Qin C, Li J, Yin C. 2014. miR-154 inhibits prostate cancer cell proliferation by targeting CCND2. *Urol Oncol* 32:e39–e16. <http://dx.doi.org/10.1016/j.urolonc.2012.11.013>.
  42. Khetani SR, Bhatia SN. 2008. Microscale culture of human liver cells for drug development. *Nat Biotechnol* 26:120–126. <http://dx.doi.org/10.1038/nbt1361>.
  43. Rheinwald JG, Green H. 1975. Serial cultivation of strains of human epidermal keratinocytes: the formation of keratinizing colonies from single cells. *Cell* 6:331–343. [http://dx.doi.org/10.1016/S0092-8674\(75\)80001-8](http://dx.doi.org/10.1016/S0092-8674(75)80001-8).
  44. Sui Y, Zhao X, Speed TP, Wu Z. 2009. Background adjustment for DNA microarrays using a database of microarray experiments. *J Comput Biol* 16:1501–1515. <http://dx.doi.org/10.1089/cmb.2009.0063>.
  45. Krämer A, Green J, Pollard J, Jr, Tugendreich S. 2014. Causal analysis approaches in ingenuity pathway analysis. *Bioinformatics* 30:523–530. <http://dx.doi.org/10.1093/bioinformatics/btt703>.
  46. Racanelli V, Rehermann B. 2006. The liver as an immunological organ. *Hepatology* 43(2 Suppl 1):S54–S62.